



Chemical Composition of Indoor and Outdoor Atmospheric Particles at Emperor Qin's Terra-cotta Museum, Xi'an, China

Jun-ji Cao^{1,5*}, Hua Li^{1,4}, Judith C. Chow², John G. Watson², Shuncheng Lee³, Bo Rong⁴, Jun-gang Dong⁶, Kin-fai Ho¹

¹ SKLLQG, Institute of Earth Environment, Chinese Academy of Sciences, China

² Division of Atmospheric Sciences, Desert Research Institute, Reno, USA

³ Department of Civil and Structural Engineering, The Hong Kong Polytechnic University, Hong Kong, China

⁴ Emperor Qin's Terra-cotta Warriors and Horses Museum, Xi'an, China

⁵ Institute of Global Environmental Change, Xi'an Jiaotong University, Xi'an, China

⁶ Xi'an University of Architecture and Technology, Xi'an, China

ABSTRACT

Indoor particles and microclimate were measured in summer (August 2004) and winter (January 2005) periods inside and outside Emperor Qin's Terra-Cotta Museum in Xi'an, China. Indoor temperature ranged from 21.9°C to 32.4°C in summer and from 0°C to 5.3°C in winter. Relative humidity varied from 56% to 80% in summer and from 48% to 78% in winter. The number concentrations of particles were lower (0.3–1.0 µm) in summer, and were higher (1.0–7.0 µm) in winter. The average indoor PM_{2.5} and TSP concentrations were 108.4 ± 30.3 µg/m³ and 172.4 ± 46.5 µg/m³ in summer and were 242.3 ± 189.0 µg/m³ and 312.5 ± 112.8 µg/m³ in winter, respectively. Sulfate, organic matter, and geological material dominated indoor PM_{2.5}, followed by ammonium, nitrate, and elemental carbon. Several milligram of sulfate particles can be deposited in the museum per square meter each year based on the dry deposition estimate. High concentrations of acidic particles suspended inside the museum and their depositions have high risk for the erosion of the terra-cotta figures.

Keywords: Terra-cotta museum; Indoor air quality; Chemical composition; Acidic particles.

INTRODUCTION

Air quality in museums is important to the preservation of rare antiquities (Thomson, 1965; Baer and Banks, 1985; Brimblecombe, 1990; Nazaroff *et al.*, 1990; Oddy, 1994; DeBock *et al.*, 1996) with damage being reported in the mid-19th century at British Art Gallery (Broughton, 1857; Speirs, 1892). Since the 1980s, a series of indoor air studies in museums have been carried out in developed countries such as Italy, Austria, Belgium, UK, and USA (Ligocki *et al.*, 1990; Nazaroff *et al.*, 1990; Grosjean *et al.*, 1992; Brimblecombe *et al.*, 1999; Camuffo *et al.*, 1999, 2001; Gysels *et al.*, 2002; Worobiec *et al.*, 2008). China has more than 2,000 museums containing artifacts from its 7,000 years' history (<http://www.sach.gov.cn/>), but little attention is paid regarding air quality and its effects on Chinese museums except for a study on the Yungang cave pollution (Christoforou *et al.*, 1996, 1999).

Emperor Qin's Terra-cotta Museum is one of China's best-known museums located 30 km east of Xi'an (34°44'N, 109°49'E), attracting more than 2 million visitors per year. It contains more than 7,000 pottery soldiers, horses, chariots, and weapons manufactured in the Qin Dynasty (208–246 BC), of which ~1400 figures have been excavated, restored, and put on display. Since they were put on display in 1979, changes in their appearance have been observed, including changes in color, pitting, and reeling of the surfaces. These changes could be caused, in part, by high air pollutant concentrations inside the museum enclosure that might result from the infiltration of high outdoor air pollutants (Cao *et al.*, 2005, 2009; Shen *et al.*, 2009). This is a comprehensive report of indoor and outdoor particulate matter (PM) concentrations and chemical compositions inside and outside of museum enclosure.

EXPERIMENTAL

Indoor and Outdoor Sampling

Three enclosures designated Pit 1, Pit 2, and Pit 3 were built over the excavated sites from 1974 to 1994. Pit 1 (14,269 m²) was built first and contains 1,087 terra-cotta

* Corresponding author. Tel.: 86-29-8832-6488;
Fax: 86-29-8832-0456
E-mail address: cao@loess.llqg.ac.cn

warriors. Pit 1 is similar to a large aircraft hanger with no environmental controls and ample ventilation with outside air. Samples were taken inside and outside of Pit 1, as shown in Fig. 1. Indoor samples were located at ~1.0 m above ground level in the statue restoration in the back of the museum (Fig. 2). The outdoor samples were located in rooftop of a two-story building near the Pit 1 (Fig. 1).

PM_{2.5} and TSP samples were collected for 24-hours at 5 L/min with a mini-vol sampler (Airmetrics, Springfield, OR, USA) on 47 mm Whatman quartz-fiber filters (QM-A, Whatman, Clifton, NJ, USA) from August 11–17, 2004 to January 7–14, 2005 (Cao *et al.*, 2003). Quartz-fiber filters were pre-heated at 900°C for 3 hours to remove the residual carbon. Particle number concentrations were

measured using a Metone six Channel Particle Counter (Metone Instruments Inc., USA) in various ranges of 0.3–0.7, 0.7–1.0, 1.0–2.0, 2.0–3.0, 3.0–7.0, and > 7.0 μm, respectively. A Q-Trak monitor (Model 8551, TSI Inc., Shoreview, MN, USA) measured 15-min average temperature, relative humidity (RH), and carbon dioxide (CO₂) on three days during both seasons.

Mass Analysis

Quartz-fiber filters were analyzed gravimetrically for mass concentrations on a Sartorius MC5 electronic microbalance with ± 1 μg sensitivity (Sartorius, Göttingen, Germany) after 24-hour equilibration at temperature between 20 and 23°C and RH between 35 and 45%. Each

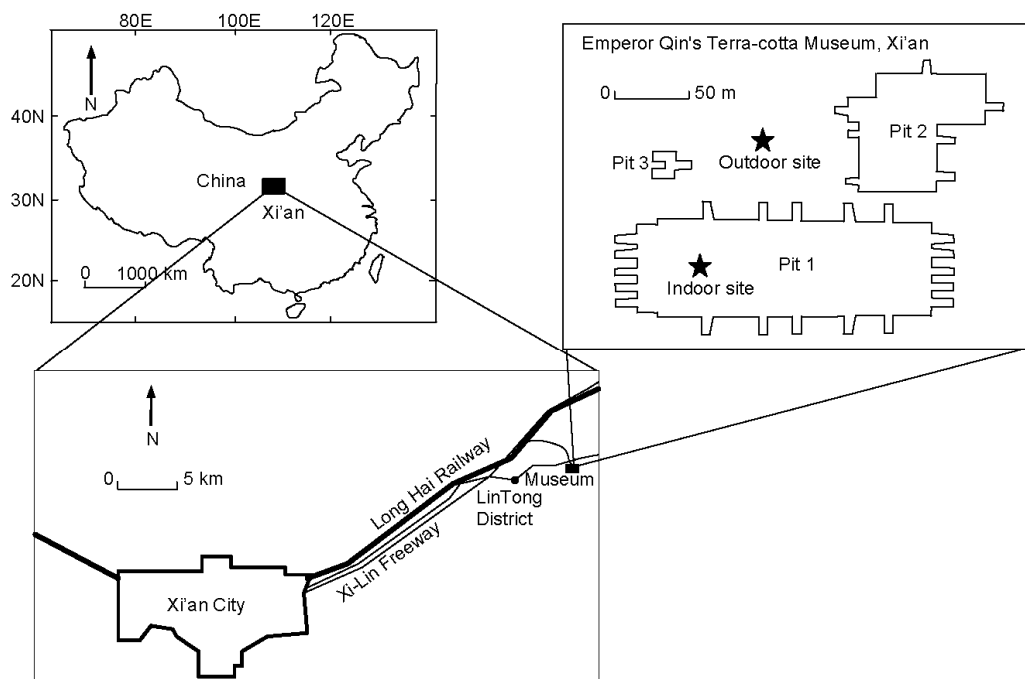


Fig. 1. Locations of the sampling sites inside and outside of the Emperor Qin's Terra-cotta Museum in Xi'an, China.



Fig. 2. Observation site inside the museum.

filter was weighed at least three times before and after samplings, and the net mass was obtained by subtracting the difference between the averaged pre- and post-sampling weights.

Elemental Analysis

Filters were analyzed for 15 elements (S, K, Ti, V, Mn, Fe, Ni, Cu, Zn, As, Se, Br, Sr, Zr, and Pb) by PIXE (Proton-induced X-ray emission spectroscopy) using 2.5 MeV protons with a 10 nA beam current through a 1.7×2 MV accelerator, and thin-film calibration standards (MicroMatter Co., Oregon) (Zhang *et al.*, 2002). Blank filter background spectra were subtracted prior to peak integration. Eight standard reference material samples from the National Bureau of Chemical Exploration Analysis, China showed reasonable precision ($< 10\%$) and accuracy ($< 15\%$).

Ion Analysis

After PIXE, 25% of the filter were removed and extracted in 10 ml of high-purity water. Six major ionic species (NH_4^+ , K^+ , Mg^{2+} , Ca^{2+} , NO_3^- , and SO_4^{2-}) were measured by DX600 ion chromatography (Dionex Inc., Sunnyvale, CA, USA) (Chow and Watson, 1999). A CS12 column (150×4 mm) and an AS14 column (150×4 mm) were used for cation and anion analysis, respectively. Field blank levels were averaged, subtracted, and standard deviations were propagated to the measurement precisions. Minimum detection limits (MDLs) were $15 \mu\text{g/L}$ for NH_4^+ , K^+ , Mg^{2+} , Ca^{2+} , and NO_3^- ; and $20 \mu\text{g/L}$ for SO_4^{2-} . Ten percent of the samples were submitted for replicate analyses. Relative standard deviations of replicate analyses were 0.6–2.5% for NO_3^- , 0.04–2.3% for SO_4^{2-} , 1.4–1.8% for NH_4^+ , and 2.3–3.6% for K^+ , 0.7–3.2% for Mg^+ , and 0.5–2.1% for Ca^{2+} .

Organic Carbon and Elemental Carbon Analyses

0.5 cm^2 punch from each quartz filter was analyzed for

organic carbon (OC) and elemental carbon (EC) by the IMPROVE thermal/optical protocol (Chow *et al.*, 1993) using a Desert Research Institute (DRI, Reno, NV, USA) Model 2001 thermal/optical carbon analyzer (Atmoslytic Inc., Calabasas, CA, USA). Quality assurance/quality control (QA/QC) procedures were described by Cao *et al.* (2003).

RESULTS AND DISCUSSION

Microclimate and CO_2

During summer, the difference between maximum and minimum daily temperatures was 3.2°C on August 15, 5.1°C on August 11, and 8.0°C on August 16 (Fig. 3). The daily average indoor temperature was 26.2°C , ranging from 21.9 to 32.4°C . The maximum temperature of 32°C was recorded from 13:40 to 15:40 on August 11. Average daily indoor temperature ranged from 0 to 5.3°C during winter. With the highest temperature of 5.3°C occurred from 13:00 to 15:00 and low temperatures occurred between 1:00 and 3:00.

Indoor RH was similar during summer and winter (Fig. 3). RH typically varied between 56 and 80%, with an average of 70.8% during summer, and between 48 and 78% in winter, with an average of 64%, consistent with the result of Zhang *et al.* (1997). Even though the museum is located in a semi-arid region of China, with an annual precipitation of 550 mm, the average indoor RH still reaches 70% during summer and 60% during winter. These levels are 15–20% higher than those measured at the Sainsbury Centre for Visual Arts, UK (Brimblecombe *et al.*, 1999), and Correr museum, Italy (Camuffo *et al.*, 1999).

Excess indoor CO_2 indicates exhaled breath from museum visitors, which range from 2322 to 8393 visitors/day. As shown in Fig. 3, CO_2 varied from 453 ppm to 741 ppm with an average of 534 ppm in summer and from 383 to 500 ppm with an average of 430 ppm in winter. Assuming an outdoor level of 380 ppm, near the minimum

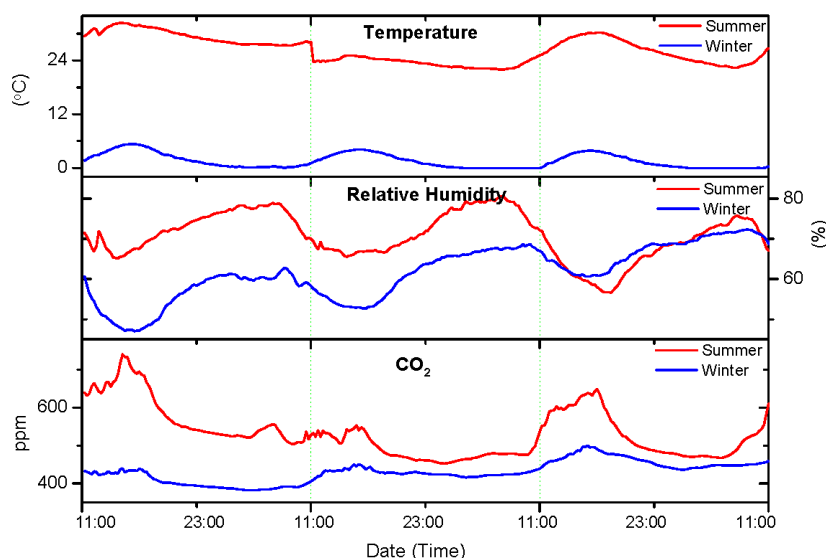


Fig. 3. 15-min average of temperature, RH, and indoor CO_2 variations for three days in summer and winter.

of 383 ppm for indoor measurement, the average CO₂ from visitors was 155 ppm in summer and 51 ppm in winter. The summer/winter CO₂ ratio of 3.0 was similar to the summer/winter visitor number ratio of 3.6.

Size-separated Number Concentrations of Indoor Particles

Fig. 4 displays the size-segregated number concentrations of indoor particles observed on August 11, 15, and 16 in summer and January 8, 10, and 12 in winter. There were 7.1×10^5 particles/cm³ in summer and 4.2×10^5 particles/cm³ in winter for 0.3 μm particles, 5.6×10^5 particles/cm³ in summer and 4.1×10^5 particles/cm³ in winter for 0.7 μm particles, respectively. For the particles with 1.0–7.0 μm, there were 2.2×10^5 , 1.2×10^4 , 3.8×10^3 , 5.8×10^3 particles/cm³ in summer, and 2.6×10^5 , 1.8×10^4 , 5.6×10^3 , 7.4×10^3 particles/cm³ in winter, respectively, for 1.0, 2.0, 3.0, and 7.0 μm particles. The ratios of particle number concentrations in winter relative to summer is 0.6, 0.7, 1.2, 1.5, 1.4, 1.3, for particle radius of 0.3, 0.7, 1.0, 2.0, 3.0, and 7.0 μm, respectively, which indicated that the small particles in the range of 0.3–0.7 μm were higher in summer, and large particles in the range of 1.0–7.0 μm were higher in winter. All the particles showed a distinct diurnal variation with a maximum during the daytime, and minimum at night, indicating a correlation with the trend of increasing tourist flow as reflected by the CO₂ levels (Figs. 3 and 4).

PM Chemical Composition

Average indoor PM_{2.5} concentrations were 108.4 ± 30.3 μg/m³ in summer and 242.3 ± 189.0 μg/m³ in winter (Table 1). Average indoor TSP concentrations were 172.4 ± 46.5 μg/m³ in summer and 312.5 ± 112.8 μg/m³ in winter, while the average outdoor TSP concentrations were 226.0 ± 104.2 μg/m³ in summer and 367.6 ± 141.5 μg/m³ in winter. This result shows that the indoor PM_{2.5} accounted for majority of total particles, with 62.9% in summer and 77.5% in winter, respectively. The indoor TSP is smaller than the outdoor TSP, accounting for 76.3% (summer) and 85.0% (winter) of outdoor TSP, respectively. The higher

concentrations of winter outdoor TSP implied that winter outdoor particles have more impact on indoor particle concentrations than summer outdoor particles. The average mass concentrations of PM in winter were 1.6–2.2 times compared with those in summer for PM_{2.5} and TSP (Table 1). All daily PM_{2.5} concentrations exceed 35 μg/m³, the U.S. 24-hour National Ambient Air Quality Standards (NAAQS) limit. The average indoor TSP (172.4 μg/m³) in 2004 was less than that (430 μg/m³) measured in the summer of 1993, but the TSP in winter of 2004 (312.5 μg/m³) was similar to the measure in the winter of 1993 (340 μg/m³) (Zhang, 1997).

Elemental Composition

The highest concentration of the 15 elements was sulfur, for the cases of both indoors and outdoors, suggesting the heavy influence of anthropogenic sources. The average S concentration reached 10.4 to 12.9 μg/m³ for indoors and 11.6 μg/m³ for outdoors in summer and 17.1 to 20.6 μg/m³ for indoors and 23.5 μg/m³ for outdoors in winter. Average S concentrations in winter were 1.6–2.0 times compared with those in summer for PM_{2.5} and TSP. The indoor TSP S concentrations were one order of magnitude higher than the S concentrations measured in four European museums (Camuffo *et al.*, 2001). The element K concentrations in winter were about 3 times higher than those in summer for PM_{2.5} and TSP, pointed to the influence of biomass burning from domestic cooking and heating in winter around the museum. Other element concentrations in winter were similar or 1–2 times higher than those in summer.

Enrichment factors of each element are summarized in Table 2 relative to crustal rock using Fe (Taylor and McLennan, 1985) as a reference element.

$$EF = (X/Fe)_{\text{air}} / (X/Fe)_{\text{crust}} \quad (1)$$

where EF is the enrichment factor of element X, $(X/Fe)_{\text{air}}$ is the concentration ratio of X to Fe in the PM samples, and $(X/Fe)_{\text{crust}}$ is the average concentration ratio of X to Fe in crustal rock.

If EF-value is approaching unity, suspended dust is

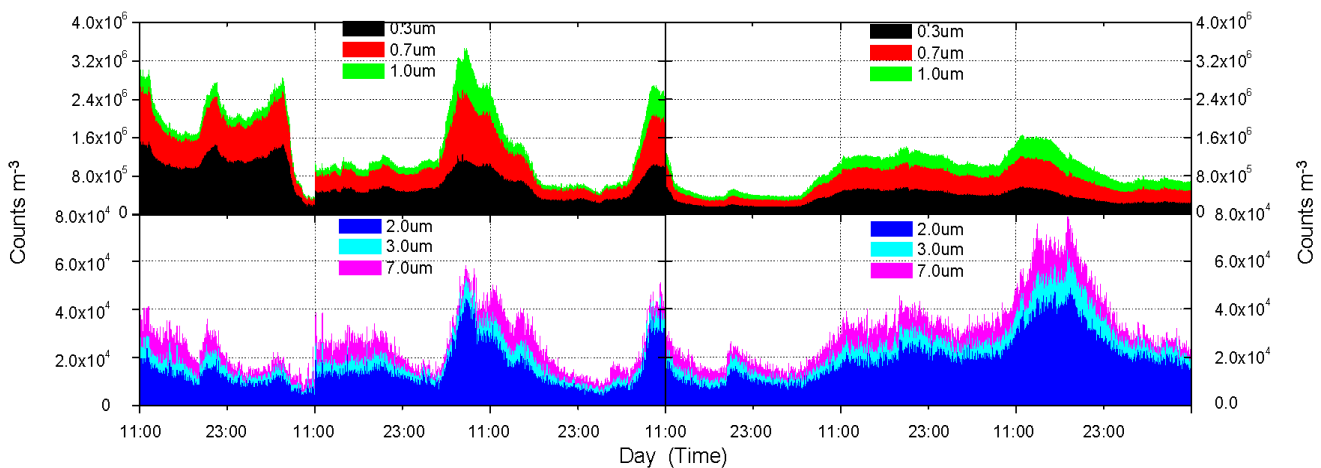


Fig. 4. Number size distributions of indoor particles for three days in summer and winter.

Table 1. Statistical summary of 24-hour PM_{2.5} and TSP chemical composition for samples acquired over summer and winter periods, indoors and outdoors at the Emperor Qin's Terra-Cotta Warriors and Horses Museum in Xi'an, China.

	Indoor PM _{2.5}		Indoor TSP		Outdoor TSP	
	Summer	Winter	Summer	Winter	Summer	Winter
Mass	108.4 ± 30.3	242.3 ± 189.0	172.4 ± 46.5	312.5 ± 112.8	226.0 ± 104.2	367.6 ± 141.5
OC	17.6 ± 2.2	41.7 ± 27.8	23.9 ± 4.2	49.6 ± 19.9	26.8 ± 3.0	56.8 ± 23.6
EC	3.9 ± 0.6	7.7 ± 5.7	5.4 ± 1.2	9.8 ± 3.7	6.6 ± 0.8	11.8 ± 4.1
NO ₃ ⁻	8.0 ± 4.1	27.2 ± 20.5	11.8 ± 6.1	33.5 ± 12.2	13.5 ± 8.4	38.1 ± 18.2
SO ₄ ²⁻	36.6 ± 14.5	58.9 ± 45.0	43.1 ± 18.1	71.1 ± 32.0	36.4 ± 19.1	81.5 ± 43.7
NH ₄ ⁺	10.3 ± 4.6	22.3 ± 17.9	10.9 ± 5.0	26.7 ± 12.4	6.6 ± 4.6	28.6 ± 16.7
Mg ²⁺	0.1 ± 0.1	0.4 ± 0.3	0.4 ± 0.2	0.6 ± 0.3	0.9 ± 0.6	0.9 ± 0.3
Ca ²⁺	1.54 ±	2.2 ± 1.9	4.7 ± 1.0	3.3 ± 1.4	9.5 ± 6.4	6.8 ± 3.3
K ⁺	1.1 ± 0.4	3.8 ± 2.4	1.5 ± 0.5	4.3 ± 1.5	1.5 ± 1.0	4.5 ± 2.1
S	10.4 ± 4.0	17.1 ± 14.0	12.9 ± 5.4	20.6 ± 9.5	11.6 ± 6.0	23.5 ± 12.7
K	0.9 ± 0.4	4.2 ± 3.0	1.4 ± 0.3	5.5 ± 1.9	1.6 ± 0.8	6.5 ± 2.3
Ti	65.2 ± 21.4	162.7 ± 190.3	234.5 ± 97.8	255.9 ± 133.9	305.3 ± 145.2	500.7 ± 182.1
V	4.4 ± 3.5	13.3 ± 10.5	7.8 ± 5.4	13.7 ± 12.4	10.9 ± 6.4	17.9 ± 7.3
Mn	35.5 ± 13.5	104.3 ± 66.3	55.4 ± 12.6	138.3 ± 57.5	96.3 ± 52.3	173.4 ± 42.6
Fe	459.3 ± 136.9	1105.8 ± 1447.9	1707.6 ± 361.9	2148.5 ± 1064.7	2842.6 ± 1547.8	3875.5 ± 1273.5
Ni	6.4 ± 5.9	13.1 ± 12.6	21.7 ± 8.2	17.9 ± 11.6	31.8 ± 20.9	28.9 ± 14.4
Cu	7.3 ± 2.1	5.3 ± 2.6	12.1 ± 1.0	13.4 ± 16.8	16.3 ± 4.6	12.7 ± 2.6
Zn	305.0 ± 183.8	603.3 ± 581.1	378.3 ± 203.4	697.0 ± 349.3	728.8 ± 612.1	842.8 ± 486.2
As	19.8 ± 6.1	63.2 ± 55.2	18.3 ± 15.0	67.0 ± 29.9	24.7 ± 15.2	56.0 ± 33.0
Se	11.6 ± 7.7	10.6 ± 6.3	14.5 ± 11.5	11.6 ± 8.3	24.9 ± 17.9	8.0 ± 5.2
Br	14.1 ± 13.6	34.7 ± 30.8	14.3 ± 10.6	44.9 ± 26.6	23.7 ± 22.9	46.2 ± 23.3
Sr	10.3 ± 9.7	24.8 ± 21.2	43.3 ± 15.3	36.2 ± 24.2	44.9 ± 28.5	104.2 ± 87.9
Zr	127.9 ± 33.7	123.0 ± 38.0	126.7 ± 47.7	123.6 ± 25.4	111.5 ± 42.1	146.9 ± 44.4
Pb	154.0 ± 75.2	461.0 ± 312.8	204.3 ± 86.1	609.6 ± 243.9	287 ± 181.1	762.1 ± 337.8

^a Unit: from mass to K, µg/m³; from Ti to Pb, ng/m³; ^b -- the element was not detected in the filter.

Table 2. Enrichment factor (relative to Fe) of selected element.

	Summer			Winter		
	Indoor PM _{2.5}	Indoor TSP	Outdoor TSP	Indoor PM _{2.5}	Indoor TSP	Outdoor TSP
S	2163.4	699.6	395.1	3941.3	2422.2	1108.9
K	2.4	1.0	0.7	6.9	3.9	2.1
Ti	1.8	1.6	1.4	2.2	1.4	1.5
V	6.8	2.7	3.9	13.2	3.7	2.9
Mn	4.6	1.9	2.0	8.3	4.2	2.7
Ni	28.0	23.1	19.8	32.1	13.4	12.6
Cu	25.4	10.2	12.2	17.6	8.0	4.8
Zn	336.3	105.8	121.0	328.8	205.9	102.0
As	1089.6	288.0	287.3	1912.9	982.8	350.7
Se	17186.8	6942.9	9552.7	18596.1	6931.7	1423.1
Sr	3.2	2.5	1.8	3.0	1.7	2.6
Zr	57.5	14.7	13.4	43.4	14.7	7.2
Pb	589.1	201.4	179.3	1051.4	613.4	335.3

probably the predominant source for element X. Table 2 shows that EF_{crust} values for K, Ti, Mn, and Sr in summer are all close to unity with maximum values less than 5, indicating that these elements were dominated by crustal elements. But in winter, the EF of K and Mn in indoor PM_{2.5} were larger than 5, consistent with the increasing contribution of anthropogenic sources like biomass and coal combustions. Compared to the dust-derived elements,

the EF values for S, Ni, Cu, Zn, As, Se, Zr, and Pb, are considerably larger than 5, illustrating the influence of anthropogenic sources such as industrial activities (Zn, Cu, S), coal-combustion (Se, As, S), oil combustion (Ni, S) and motor vehicle exhaust (Pb, Zn). The elements of Se, S, and As are the most enriched elements. The highest EF-value, ranging from 10³ to 10⁵, was found for Se, S, and As, suggesting the domination of coal-burning emissions

(Zhang *et al.*, 2002). A major coal-fired power plant (i.e., Baqiao Thermo Power Plant) is located ~15 km east of the museum and emits 1.6 tons of fly ash per day, which could be a major contributor of the high concentrations of Se, S, and As. Average EFs for Pb and Zn in the range of 10^2 to 10^3 are related to motor vehicle exhausts. All the EF-values of anthropogenic elements associated with the indoor $PM_{2.5}$ are large than those with the indoor TSP for both summer and winter (Table 2), implying the dominant presence of these elements in fine particles.

Water-soluble Ions

SO_4^{2-} contributions were the highest of the ionic species with average concentrations of 36.6/43.1 and 58.9/71.1 $\mu\text{g}/\text{m}^3$, in summer and winter, respectively, for indoor $PM_{2.5}$ /TSP (Table 1). About 83–85% TSP SO_4^{2-} resided in $PM_{2.5}$ fraction for in summer and winter. A high SO_4^{2-} fraction in fine mode is consistent with the observation of Gysels *et al.* (2002) in the Royal Museum of Fine Arts, Belgium. All the ionic concentrations in winter were higher than those in summer for both indoor and outdoor except TSP Ca^{2+} , implying the serious pollution in winter. Compared with the observations of Santis (1992), summer and winter SO_4^{2-} , NO_3^- , and NH_4^+ inside Xi'an museum were approximately 4–6 fold, 7–20 fold, and 8–20 fold, respectively, higher than those measured at Galleria degli Uffizi in Florence, Italy.

Eqs. (2) and (3) are used to calculate the charge balance between cation and anion. The correlations between cation and anion are summarized in Table 3.

$$\text{Cation Equivalence} = \frac{Ca^{2+}}{20} + \frac{K^+}{39} + \frac{Mg^{2+}}{12} + \frac{NH_4^+}{18} \quad (2)$$

$$\text{Anion Equivalence} = \frac{NO_3^-}{62} + \frac{SO_4^{2-}}{48} \quad (3)$$

The cation and anion concentrations measured for indoor $PM_{2.5}$ /TSP and outdoor TSP have correlation coefficients (R^2) greater than 0.9, suggesting the same origin of TSP in indoor and outdoor. The slopes of indoor $PM_{2.5}$ and TSP are larger than 1.3 in summer and close to 1.1 in winter. Since most inorganic species have been measured, the deficits of cation species indoors is consistent with the presence of a hydrogen ion (H^+), implying that the particles are acidic (Kerminen *et al.*, 2001). Acidic particles inside the museum can potentially damage antiquities. The slope 0.93 of outdoor TSP in summer is close to 1.0, consistent with cation species being neutralized in the outdoor atmosphere. High concentrations of Ca^{2+} in coarse mode contribute to the

neutralization of excess sulfuric and nitric acidic particles in summer (Table 1).

Organic and Elemental Carbon

Average OC concentrations were 17.6 ± 2.2 , 23.9 ± 4.2 , and 26.8 ± 3.0 $\mu\text{g}/\text{m}^3$ in summer, and 41.7 ± 27.8 , 49.6 ± 19.9 , and 56.8 ± 23.6 $\mu\text{g}/\text{m}^3$ in winter, respectively, for indoor $PM_{2.5}$, indoor TSP, and outdoor TSP (Table 1). The corresponding average EC concentrations were 3.9 ± 0.6 , 5.4 ± 1.2 , and 6.6 ± 0.8 $\mu\text{g}/\text{m}^3$ in summer, and 7.7 ± 5.7 , 9.8 ± 3.7 , and 11.8 ± 4.1 $\mu\text{g}/\text{m}^3$ in winter. The average OC and EC concentrations in winter were about 2 times compared with those in summer. The indoor concentrations of TSP EC in summer and winter are comparable to those measured at Sepulveda House (5.6 $\mu\text{g}/\text{m}^3$), but are higher than those measured at the Norton Simon Museum (0.67 $\mu\text{g}/\text{m}^3$) and Scott Gallery (0.16 $\mu\text{g}/\text{m}^3$) in Southern California (Nazaroff *et al.*, 1990).

The average OC/EC ratios were 4.5, 4.4, and 4.1, respectively, for indoor $PM_{2.5}$, indoor TSP, and outdoor TSP in summer, and were 5.4, 5.1, and 4.8, in winter. The slight increase of OC/EC ratios in winter may be attributed to the influence of coal combustion (Cao *et al.*, 2005) because coal combustion emitted high OC/EC ratio of carbonaceous particles.

Material Balances of $PM_{2.5}$ and TSP

The material balance approach (Solomon *et al.*, 1989) is used to estimate mass closure. Because the PIXE data does not analyze Al and Si, Fe is used to estimate the upper limit of geological material (Taylor and McLennan, 1985). As a result, the amount of geological material was calculated by

$$\text{Geological material} = (1/0.035) \times \text{Fe} \quad (4)$$

According to the study of Turpin *et al.* (2001), the amount of organic material can be determined by multiplying the amount of OC by 1.6 as expressed by Eq. (5):

$$\text{Organic material} = 1.6 \times \text{OC} \quad (5)$$

The material balances for geological material (crustal material), organic matter (OM), EC, ammonium (NH_4^+), sulfate (SO_4^{2-}), nitrate (NO_3^-) and others (as the difference between the measured mass and the sum of the major components) for indoor $PM_{2.5}$ /TSP and outdoor TSP in summer and winter, are shown in Fig. 5. For indoor $PM_{2.5}$,

SO_4^{2-} was the largest component, which accounted for 31% of the mass in summer. However, it was the second

Table 3. Cation and anion balance in indoor and outdoor aerosol samples.

	Summer		Winter	
Indoor TSP	A.E. = 1.31C.E. – 0.11	$R^2 = 0.96$	A.E. = 1.08C.E. + 0.06	$R^2 = 0.99$
Indoor $PM_{2.5}$	A.E. = 1.38C.E. – 0.05	$R^2 = 0.98$	A.E. = 1.08C.E. + 0.08	$R^2 = 1.0$
Outdoor TSP	A.E. = 0.93C.E. + 0.09	$R^2 = 0.92$	A.E. = 1.04C.E. + 0.09	$R^2 = 0.99$

Note: A.E. refers to Anion Equivalence; C.E. refers to Cation Equivalence.

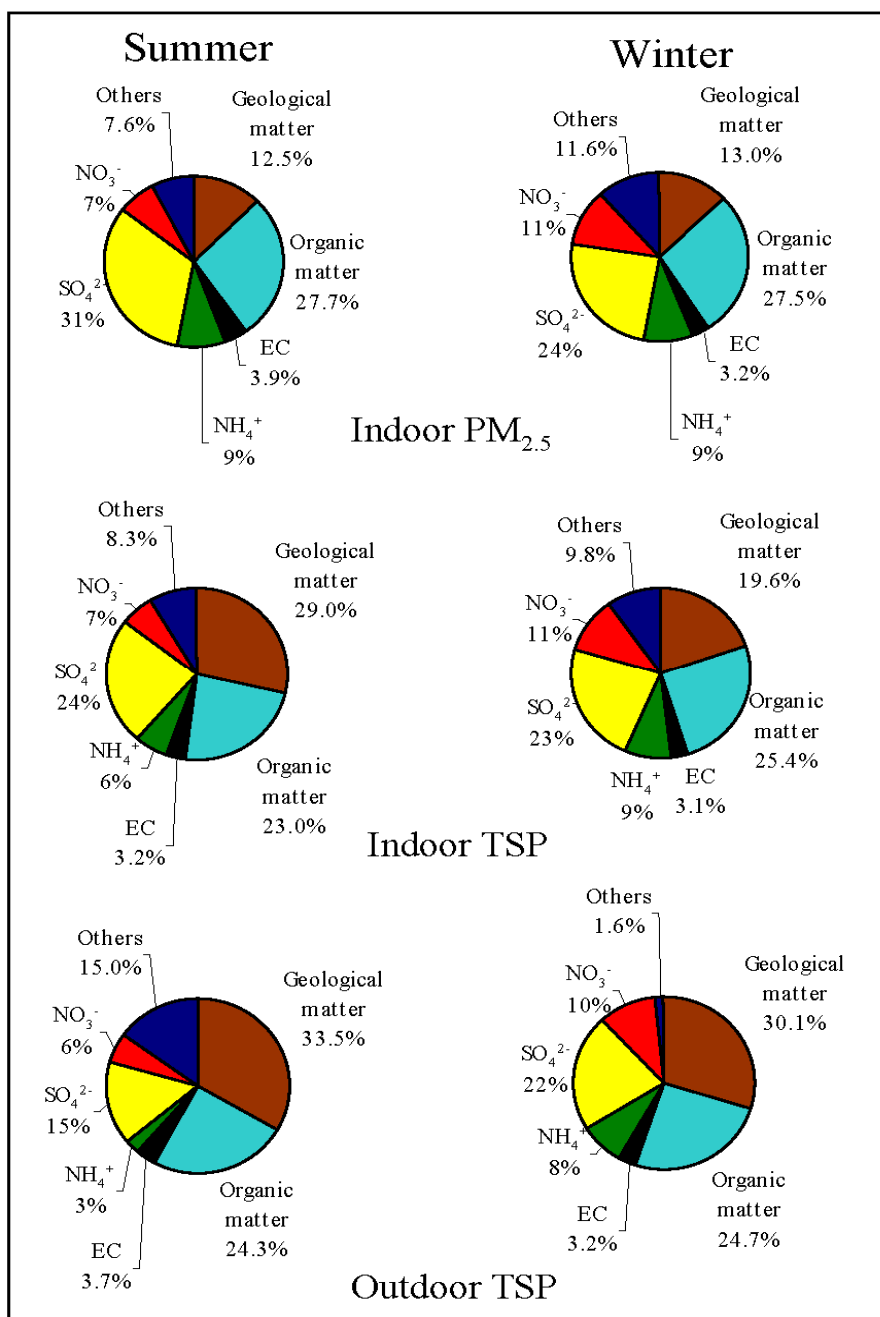


Fig. 5. Material balance charts for indoor PM_{2.5} and indoor/outdoor TSP.

largest component with 24% of the mass in winter. Higher percentage of SO₄²⁻ in summer was associated with the formation of SO₄²⁻ under high temperature and high RH (Fig. 3) as well as high photochemical activities (such as high OH radical concentrations). The percentage of OM was almost same in summer (27.7%) and winter (27.5%), and it was the second largest component in summer and became to the largest component winter. The percentage of geological material likes the share distribution of OM, i.e., it accounted for 12.5% in summer and 13% in winter with the third largest component for two seasons. NO₃⁻ accounted for 7% in summer and increased to 11% in winter, which may be due to more particulate NO₃⁻ resided

in fine particles under lower temperature in winter. The percentages of NH₄⁺ (9%) and EC (3.2–3.9%) kept stable in summer and winter.

Compared with the each individual contribution to the total mass of indoor PM_{2.5}, the contribution of geological matter was considerably higher in indoor TSP than in indoor PM_{2.5} in both summer and winter. This result is due to the fact that the contribution of coarse particles (dust) was increased as the result of the resuspension of visitors' activities in the museum. The percentage of geological matter in winter (19.6%) was less than that in summer (29%), which is owing to the fewer visitors in winter (see section 3.1).

The sum of SO_4^{2-} , NO_3^- , and NH_4^+ accounted for 47 and 44% in summer and winter, respectively, for indoor $\text{PM}_{2.5}$, and 37 and 44% in summer and winter, respectively, for indoor TSP. Thus, the high percentage (37–47%) of secondary inorganic aerosol suspended in museum air may exert potential hazard to works of art posed by the deposition of airborne particles. Gysels *et al.* (2002) showed that organic compounds, S-rich and Fe-rich particles are considered as the most harmful factor to the works of art in a museum.

EC accounted for about 3% in $\text{PM}_{2.5}$ and TSP for two seasons, which also have negative impact on culture relics because it is a catalyst to accelerate the chemical reaction of acid species and a soiling and blackening contributor to the aesthetic values of terra-cotta figures. Elemental carbon had been found to yield perceptible soiling in the three southern California museums after accumulated on vertical surfaces (Nazaroff *et al.*, 1990). In outdoor TSP, geological material accounted for the largest components both in summer and winter. Compared with indoor $\text{PM}_{2.5}$, the percentage of SO_4^{2-} increased from 15% in outdoor TSP to 31% in indoor $\text{PM}_{2.5}$ in summer, while it had similar level in winter. Since the Pit 1 is always open in summer and winter, the outdoor particles can penetrate into the museum easily. The large difference between indoor and outdoor of SO_4^{2-} in summer can be attributed to the formation of SO_4^{2-} in the museum rather than the transport from outside of SO_4^{2-} . There has no clear difference for the percentage of NO_3^- between indoor $\text{PM}_{2.5}$, TSP and outdoor TSP in both summer and winter (Fig. 5). However, there are some different between summer and winter. For example, NO_3^- accounted for 6–7% of the mass in summer and 10–11% of the mass in winter. This suggested that the increasing formation of NO_3^- in winter was ascribed to the regional atmospheric chemistry rather than the indoor chemistry. Similar changes can be observed for NH_4^+ with SO_4^{2-} , which can be ascribed to the accelerated conversion from

indoor NH_3 to particulate NH_4^+ in summer. Elevated NH_3 in summer may be associated with the use of fertilizers in the farmland around the museum as well as the contributions from local sanitation waste. Additional indoor ammonia can be attributed to the large emission of NH_3 from the high traffic of visitors (about 8,000 tourists per day in summer) and from the unvented indoor restrooms under high temperature. The percentage of NH_4^+ in winter was similar in indoor $\text{PM}_{2.5}$, TSP, and outdoor TSP, which can be ascribed to the regional transport. The indoor formation of NH_4^+ was reduced by the lower indoor NH_3 emissions from the frozen farmland, the deceased visitors, and the lower atmospheric temperature in winter.

I/O Ratios of Chemical Species

The indoor/outdoor (I/O) ratios for measured chemical species in TSP are illustrated in Fig. 6 to evaluate the difference between indoor and outdoor concentrations. The I/O ratios of mass, geological matter, organic matter, EC, and NO_3^- were less than or close to 1.0, which indicated the indoor sources for these species were not significant. NH_4^+ and SO_4^{2-} have high I/O ratios in summer. The I/O ratios for NH_4^+ ranged from 0.8 to 1.8 with an average of 1.2, and the I/O ratios for SO_4^{2-} varied from 0.6 to 1.8 with an average of 1.1 in summer, which demonstrated they were affected by indoor pollutant sources. As mentioned above, the formations of NH_4^+ and SO_4^{2-} inside museum were important in summer. The average I/O ratios of NH_4^+ and SO_4^{2-} decreased to 1.0 and 0.95, which implied that there was almost no indoor formation for these two species in cold season.

Deposited Estimates of SO_4^{2-} , NO_3^- , and NH_4^+

Deposition of particles can cause soiling and darkening of the appearance of art objects. In this study, we estimated the quantity of deposition for some key species, including SO_4^{2-} , NO_3^- , and NH_4^+ based on the measurements. Since

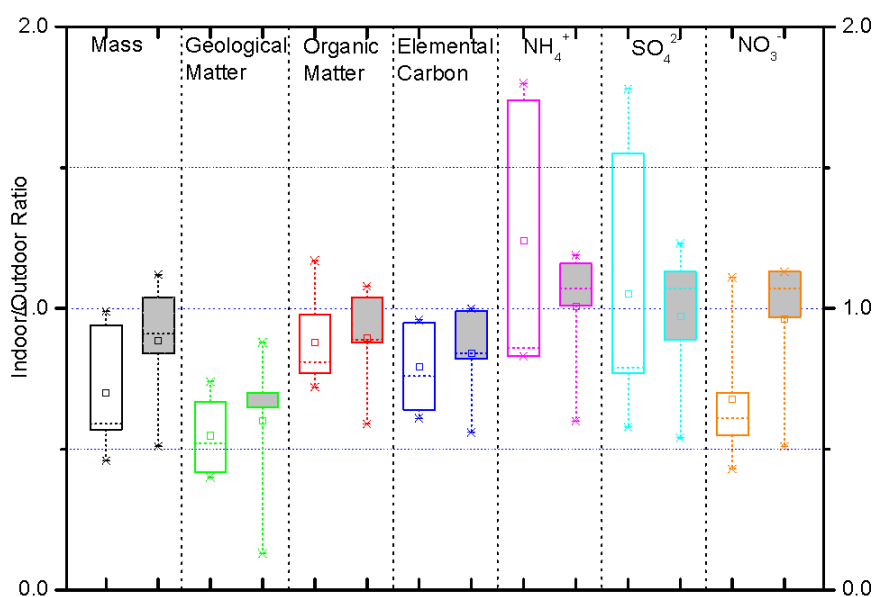


Fig. 6. I/O ratios for TSP mass and its major components (empty refer to summer, shade ref to winter).

we didn't measure the deposition velocities of these species, we used the values from other studies. Ligocki *et al.* (1990) obtained the deposition velocities of SO_4^{2-} , NO_3^- , and NH_4^+ were $38\text{--}290 \times 10^{-6}$, $110\text{--}705 \times 10^{-6}$, and $4.6\text{--}29 \times 10^{-6}$ m/s, respectively, in summer, and $74\text{--}1060 \times 10^{-6}$ m/s, $90\text{--}260 \times 10^{-6}$ m/s, and no value, respectively, in winter, based on five museums studies in Southern California. The dry deposition flux (F) for a species can be calculated as the product of its concentration (Ca) and deposition velocity (Vd):

$$F = Ca \times Vd \quad (6)$$

Based on the measured TSP concentrations of SO_4^{2-} , NO_3^- , and NH_4^+ in summer and winter, the calculated the deposition fluxes of SO_4^{2-} , NO_3^- , and NH_4^+ were 52–394, 41–279, and 1.6–10 mg/m²/yr, respectively, in summer, and 166–2377, 95–274, 4–24 mg/m²/yr (using the deposition velocity in summer for calculation), respectively, in winter. From the above calculations, the deposition of SO_4^{2-} particles was up to several mg per square meter in the museum each year, which can induce chemical reaction in the surface of art objects. Hu *et al.* (2006) observed the erosion evidence from the deposition of sulfate-rich particles in the surface of terra-cotta figures.

CONCLUSIONS

Through the investigation of air quality in the Emperor Qin's Terra-cotta Museum, Xi'an, China we can obtained the following findings. Fine particle and TSP levels were considerably high in both summer and winter. Sulfate, nitrate, carbon and geological matter were important components of particulate matter. Most of the indoor particles can be resulted from outdoor activities. Thus, high concentrations of acidic particles suspended inside the museum and their depositions have high risk for the erosion of the terra-cotta figures, especially under high variation of temperate and RH. In order to protect these culture relics, hazard removal devices should be considered to install for reducing the gas precursors like SO_2 and NH_3 in the future.

ACKNOWLEDGEMENTS

This study is supported by the projects of Natural Science Funding of China (NSFC 40875089, 40925009) and Chinese Academy of Sciences (KZCX2-YW-BR-10, O929011018), Desert Research Institute, the Nazir and Mary Ansari Foundation.

REFERENCE

- Baer, N.S. and Banks, P.N. (1985). Indoor Air Pollution: Effects on Cultural and Historical Materials. *Int. J. Mus. Mgmt. Cur.* 4: 9–20.
- Brimblecombe, P. (1990). The Composition of Museum Atmospheres. *Atmos. Environ.* 24: 1–8.
- Brimblecombe, P., Blades, N., Camuffo, D., Sturaro, G., Valentino, A., Gysels, K., Van Grieken, R., Busse, H.J., Kim, O., Ulrych, U. and Wieser, M. (1999). The Indoor Environment of a Modern Museum Building, the Sainsbury Centre for Visual Arts, Norwich, UK. *Indoor Air* 9: 146–164.
- Broughton, L. (1857). Report of Commission on the Site for a New National Gallery. *British Sessional Papers, House of Commons, Session 2*: 24.
- Camuffo, D., Brimblecombe, P., Van Grieken, R., Busse, H.J., Sturaro, G., Valentino, A., Bernardi, A., Blades, N., Shooter, D., De Bock, L., Gysels, K., Wieser M. and Kim, O. (1999). Indoor Air Quality at the Correr Museum, Venice, Italy. *Sci. Total Environ.* 236: 135–152.
- Camuffo, D., Van Grieken, R., Busse, H.J., Sturaro, G., Valentino, A., Bernardi, A., Blades, N., Shooter, D., Gysels, K., Deutsch, F., Wieser, M., Kim, O. and Ulrych U. (2001). Environmental Monitoring in Four European Museums. *Atmos. Environ.* 35: S127–S140.
- Cao, J.J., Lee, S.C., Ho, K.F., Fung, K., Chow, J.C. and Watson, J.G. (2006). Characterization of Roadside Fine Particulate Carbon and its Eight Fractions in Hong Kong. *Aerosol Air Qual. Res.* 6: 106–122.
- Cao, J.J., Lee, S.C., Ho, K.F., Zhang, X.Y., Zou, S.C., Fung, K., Chow, J.C. and Watson, J.G. (2003). Characteristics of Carbonaceous Aerosol in Pearl River Delta Region China during 2001 Winter Period. *Atmos. Environ.* 37: 1451–1460.
- Cao, J.J., Wu, F., Chow, J.C., Lee, S.C., Li, Y., Chen, S.W., An, Z.S., Fung, K.K., Watson, J.G., Zhu, C.S. and Liu, S.X. (2005). Characterization and Source Apportionment of Atmospheric Organic and Elemental Carbon during Fall and Winter of 2003 in Xi'an, China. *Atmos. Chem. Phys.* 5: 3127–3137.
- Cao, J.J., Zhang, T., Chow, J.C., Watson, J.G., Wu, F. and Li, H. (2009). Characterization of Atmospheric Ammonia over Xi'an, China. *Aerosol Air Qual. Res.* 9: 277–289.
- Chow, J.C. and Watson, J.G. (1999). In *Elemental Analysis of Airborne Particles*, Vol. 1, Ion Chromatography in Elemental Analysis of Airborne Particles, Landsberger, S. and Creatchman, M. (Eds.), Gordon and Breach Science, Amsterdam, p. 97–137.
- Chow, J.C., Watson, J.G., Chen, L.W.A., Arnott, W.P. and Moosmüller, H. (2004). Equivalence of Elemental Carbon by Thermal/Optical Reflectance and Transmittance with Different Temperature Protocols. *Environ. Sci. Technol.* 38: 4414–4422.
- Christoforou, C.S., Salmon, L.G. and Cass, G.R. (1996). Fate of Atmospheric Particles within the Buddhist Cave Temples at Yungang China. *Environ. Sci. Technol.* 30: 3425–3434.
- Christoforou, C.S., Salmon, L.G. and Cass, G.R. (1999). Passive Filtration of Airborne Particles from Buildings Ventilated by Natural Convection: Design Procedures and a Case Study at the Buddhist Cave Temples at Yungang, China. *Aerosol Sci. Technol.* 30: 530–544.
- De Bock, L.A., Van Grieken, R.E., Camuffo, D. and Grime, G.W. (1996). Microanalysis of Museum Aerosols to Elucidate the Soiling of Paintings: Case of the Correr Museum, Venice, Italy. *Environ. Sci. Technol.* 30: 3341–3350.

- Gray, H.A., Cass, G.R., Huntzicker, J.J., Heyerdahl, E.K. and Rau, J.A. (1986). Characteristics of Atmospheric Organic and Elemental Carbon Particle Concentrations in Los Angeles. *Environ. Sci. Technol.* 20: 580–589.
- Grosjean, D., Salmon, L.G. and Cass, G.R. (1992). Fading of Organic Artists' Colorants by Atmospheric Nitric Acid: Reaction Products and Mechanisms. *Environ. Sci. Technol.* 26: 952–959.
- Gysels, K., Deutsch, F. and Grieken, R.V. (2002). Characterisation of Particulate Matter in the Royal Museum of Fine Arts Antwerp Belgium. *Atmos. Environ.* 36: 4103–4113.
- Hu, T.F., Li, X.X., Dong, J.G., Rong, B., Shen, Z.X., Cao, J.J., Lee, S.C., Chow, J.C. and Watson, J.G. (2006). Morphology and Elemental Composition of Dustfall Particles Inside Emperor Qin's Terra-cotta Warriors and Horses Museum. *China Particuology* 4: 346–351.
- Huang, H., Cao, J.J., Lee, S.C., Zou, C.W., Chen, X.G. and Fan, S.J. (2007). Spatial Variation and Relationship of Indoor/Outdoor PM_{2.5} at Residential Homes in Guangzhou City, China. *Aerosol Air Qual. Res.* 7: 518–530.
- Kerminen, V.M., Hillamo, R., Teinilä, K., Pakkanen, T., Allegrini, I. and Sparapani, R. (2001). Ion Balances of Size-resolved Tropospheric Aerosol Samples: Implications for the Acidity and Atmospheric Processing of Aerosols. *Atmos. Environ.* 35: 5255–5265.
- Ligocki, M.P., Liu, H.I.H., Cass, G.R. and John, W. (1990). Measurements of Particle Deposition Rates Inside Southern California Museums. *Aerosol Sci. Technol.* 13: 85–101.
- Nazaroff, W.M., Salmon, L.G., and Cass, G.R. (1990). Concentration and Fate of Airborne Particles in Museums. *Environ. Sci. Technol.* 24: 66–77.
- Oddy, W.A. (1994). Chemistry in the Conservation of Archaeological Materials. *Sci. Total Environ.* 143: 121–126.
- Santis, F.D., Palo, V.D. and Allegrini, I. (1992). Determination of some Atmospheric Pollutants Inside a Museum: Relationship with the Concentration Outside. *Sci. Total Environ.* 127: 211–223.
- Shen, Z.X., Cao, J.J., Tong, Z., Liu, S.X., Siva Sankara Reddy, L., Han, Y.M., Zhang, T. and Zhou, J. (2009). Chemical Characteristics of Submicron Particles in Winter in Xi'an. *Aerosol Air Qual. Res.* 9: 80–93.
- Solomon, P.A., Fall, T., Salmon, L., Cass, G.R., Gray, H.A. and Davidson, A. (1989). Chemical Characteristics of PM₁₀ Aerosols Collected in the Los Angeles Area. *J. Air Pollut. Contr. Assoc.* 39: 154–163.
- Speirs (1892). An Improved Method or Means of Preserving Oil Paintings, Water Colour Drawings, Engravings, Photographs, Prints, and Printed Matter from Atmospheric Deterioration and from Decay. Patent Number 6556, 1892, Her Majesties Stationery Office, London, UK.
- Taylor, S.R. and McLennan, S.M. (1985). *The Continental Crust: Its Composition and Evolution*, Oxford. Blackwell p. 315.
- Thomson, G. (1965). Air Pollution – A Review for Conservation Chemists. *Stud. Conserv.* 10: 147–167.
- Turpin, B.J. and Lim, H.J. (2001). Species contributions to PM_{2.5} Mass Concentrations: Revisiting common Assumptions for Estimating Organic Mass. *Aerosol Sci. Technol.* 35: 602–610.
- Watson, J.G., Chow, J.C., and Chen, L.W.A. (2005). Summary of Organic and Elemental Carbon/Black Carbon Analysis Methods and Intercomparisons. *Aerosol Air Qual. Res.* 5: 65–102.
- Worobiec, A., Samek, L., Karaszkiwicz, P., Kontozova-Deutsch, V., Stefaniak, E.A., Van Meel, K., Krata, A., Bencs, L., and Van Grieken, R. (2008). A Seasonal Study of Atmospheric Conditions Influenced by the Intensive Tourist Flow in the Royal Museum of Wawel Castle in Cracow, Poland. *Microchem. J.* 90: 99–106.
- Zhang, X.Y., Cao, J.J., Li, L.M., Arimoto, R., Cheng, Y., Huebert, B. and Wang, D. (2002). Characterization of Atmospheric Aerosol over Xi'an in the South Margin of the Loess Plateau, China. *Atmos. Environ.* 36: 4189–4199.
- Zhang, Z.J. (1997). In *Conservation of Terra-cotta Warriors and Horses*, Study on Environmental Quality of Emperor Qin's Terra-cotta Museum, Xi'an, Zhang, Z.J. (Eds.), Shaanxi People Press p. 1–49.

Received for review, October 10, 2010

Accepted, December 9, 2010